JOC Article

DFT Study of Pericyclic and Pseudopericyclic Thermal Cheletropic Decarbonylations. Evaluation of Magnetic Properties

Jesús Rodríguez-Otero,*,† Enrique M. Cabaleiro-Lago,‡ Jose M. Hermida-Ramón,§ and Angeles Peña-Gallego†

Departamento de Química Física, Facultade de Química, Universidade de Santiago de Compostela, Avda das Ciencias s/n, 15782 Santiago de Compostela, Spain, Departamento de Química Física, Facultade de Ciencias, Universidade de Santiago, Campus de Lugo, Avda Alfonso X El Sabio s/n, 27002 Lugo, Spain, and Departamento de Química Física, Facultade de Ciencias, Universidade de Vigo, Campus Lagoas Marcosende, 36200 Vigo, Galicia, Spain

qftjesus@usc.es

Received April 24, 2003

A comprehensive B3LYP/6-31G** study of various thermal cheletropic decarbonylations was conducted. The complete pathway for each reaction was determined, and changes in magnetic susceptibility and its anisotropy were monitored with a view to estimating the aromatization associated to each process. This information, together with the energy and structural results, allowed us to clarify cases that are not clearly pseudopericyclic or pericyclic from previous work. Also, our results reveal that pericyclic reactions involve no disconnection in the cyclic array of overlapping orbitals. Therefore, a pseudopericyclic reaction involves at least one such disconnection. In any case, pseudopericyclic reactions involving two disconnections exhibit much clearer features, which facilitates their classification.

Introduction

According to the original definition of Lemal a pseudopericyclic reaction is a concerted transformation whose primary changes in bonding encompass a cyclic array of atoms, at one (or more) of which nonbonding and bonding atomic orbitals interchange roles.[1] The role interchange means a "disconnection" in the cyclic array of overlapping orbitals because the atomic orbitals switching functions are mutually orthogonal. Hence, pseudopericyclic reactions cannot be orbital symmetry forbidden.

Following this definition by Lemal, pseudopericyclic reactions fell into oblivion until Birney[2−8] first and several other authors[9−13] later revived interest in them by showing that a number of organic syntheses involve this type of process. Although Lemal's definition is seemingly quite clear, there is some ambiguity in it as the orbital description is not unique; thus, any unit transformation of canonical molecular orbitals can be used to reproduce molecular properties. Also, most of the studies on the topic have so far focused virtually exclusively on the properties of the transition state when it would have been more advisable to monitor the whole reaction.

Therefore, no universally accepted clear-cut, absolute criterion exists for distinguishing a pseudopericyclic reaction from a normal pericyclic reaction. This has raised some controversy in classifying some reactions.[14−17] In addition to using structural criteria and natural bonding orbitals (NBOs),[18−20] we examined magnetic properties with a view to assessing aromatization during the processes. This relies on the fact that the cyclic loop of a pericyclic reaction yields an aromatic transition state,[21] as quantitatively confirmed for various reactions.[22−25]

† Universidade de Santiago de Compostela.
‡ Universidade de Santiago, Campus de Lugo.
§ Universidade de Vigo, Campus Lagoas Marcosende.
* Corresponding author.

(1) Ross, J. A.; Seiders, R. P.; Lemal, D. M. *J. Am. Chem. Soc.* **1976**, *98*, 4325−4327.
(2) Birney, D. M.; Wagenseller, P. E. *J. Am. Chem. Soc.* **1994**, *116*, 6262−6270.
(3) Birney, D. M. *J. Org. Chem.* **1996**, *61*, 243−251.
(4) Birney, D. M.; Ham, S.; Unruh, G. R. *J. Am. Chem. Soc.* **1997**, *119*, 4509−4517.
(5) Birney, D. M. *J. Am. Chem. Soc.* **2000**, *122*, 10917−10925.
(6) Shumway, W.; Ham, S.; Moer, J.; Whittlesey, B. R.; Birney, D. M. *J. Org. Chem.* **2000**, *65*, 7731−7739.
(7) Shumway, W. W.; Dalley, N. K.; Birney, D. M. *J. Org. Chem.* **2001**, *66*, 5832−5839.
(8) Zhou, C.; Birney, D. M. *J. Am. Chem. Soc.* **2002**, *124*, 5231−5241.
(9) Luo, L.; Bartberger, M. D.; Dolbier, W. R. J. *J. Am. Chem. Soc.* **1997**, *119*, 12366−12367.
(10) Fabian, W. M. F.; Bakulev, V. A.; Kappe, C. O. *J. Org. Chem.* **1998**, *63*, 5801−5805.
(11) Fabian, W. M. F.; Kappe, C. O.; Bakulev, V. A. *J. Org. Chem.* **2000**, *65*, 47−53.
(12) Alajarin, M.; Vidal, A.; Sanchez-Andrada, P.; Tovar, F.; Ochoa, G. *Org. Lett.* **2000**, *2*, 965−968.
(13) Rauhut, G. *J. Org. Chem.* **2001**, *66*, 5444−5448.
(14) De Lera, A. R.; Alvarez, R.; Lecea, B.; Torrado, A.; Cossio, F. P. *Angew. Chem., Int. Ed.* **2001**, *40*, 557−561.
(15) Rodríguez-Otero, J.; Cabaleiro-Lago, E. M. *Angew. Chem., Int. Ed.* **2002**, *41*, 1147−1150.
(16) De Lera, A. R.; Cossio, F. P. *Angew. Chem., Int. Ed.* **2002**, *41*, 1150−1152.
(17) Rodríguez-Otero, J.; Cabaleiro-Lago, E. M. *Chem. Eur. J.* **2003**, *9*, 1837−1843.
(18) Foster, J. P.; Weinhold, F. *J. Am. Chem. Soc.* **1980**, *102*, 7211.
(19) Reed, A. D.; Curtiss, L. A.; Weinhold, F. *Chem. Rew.* **1988**, *88*, 899.
(20) Glendening, E. D.; Reed, A. E.; Carpenter, J. E.; Weinhold, F. *NBO 3.1 Program Manual*, 1988.
(21) Zimmermann, H. E. *Acc. Chem. Res.* **1971**, *4*, 272.

10.1021/jo034526o CCC: $25.00
Published on Web 10/23/2003

Thus, Herges et al. showed that, in the vicinity of the transition state in the Diels−Alder reaction, the magnetic susceptibility (χ) and its anisotropy (χ_{anis}) exhibit well-defined minima with respect to the reactant and product.[22] On the other hand, the typical disconnection of pseudopericyclic reactions would have prevented this aromatization, as shown by our group for the unequivocally pseudopericyclic cyclization of 5-oxo-2,4-pentadienal to pyran-2-one.[17] This reaction involves the in-plane attack of the lone electron pair on the carbonyl oxygen to the electrophilic allene carbon. The way χ and, especially, χ_{anis} change along the reaction coordinate reveals that the process involves no appreciable aromatization. This clearly departs from the typical aromatization of pericyclic processes.

Another method that uses the magnetic properties is ACID (anisotropy of the current-induced density), developed recently by Herges and Geunich.[26] It has been proved that this method is very useful for the quantitative study of delocalization in molecules. Also it has been used to study several pericyclic reactions and to distinguish a coarctate reaction from a pseudocoarctate reaction.[27,28] This fact seems to indicate that this method could be useful for the study of pseudopericyclic reactions. Nevertheless, its systematic application to a substantial number of pseudopericyclic reactions is still necessary to confirm its general validity in this research field.

In one paper about pseudopericyclic reactions, Birney et al.[4] raised the following question: how many and what types of disconnections in the loop of interacting orbitals are necessary to obtain the energy benefits of a pseudopericyclic reaction pathway? To provide an answer, these authors examined various thermal cheletropic decarbonylations and concluded that two orbital disconnections suffice to allow a reaction to be pseudopericyclic and to have a roughly planar transition structure. Orbital disconnections can occur both at cumulene carbons and at atoms bearing lone electron pairs. According to Birney et al., a single disconnection may, but will not always, lead to a pseudopericyclic transition structure. However, this conclusion is in open conflict with Lemal's original definition, on the basis of which a single disconnection is enough to produce a pseudopericyclic reaction. Specifically, Birney et al. classified the thermal cheletropic reactions of Figure 1 as follows: reaction A is the prototype of a pericyclic reaction (cyclic orbital overlap); reactions B and E are pseudopericyclic with two orbital disconnections; and reactions C and D both involve a single disconnection, but the former is pericyclic whereas the latter is pseudopericyclic. This last conclusion is in clear contradiction with Lemal's original definition.

On the basis of the foregoing, in this work we conducted a comprehensive DFT study of the reactions of Figure 1. The reaction F is analogous with reaction C and had never previously been examined. In reaction F, the substitution of the oxygen atom by the nitrogen leaves an electron lone pair that is still properly oriented for the disconnection to occur; however, this reaction has the advantage that it introduces a hydrogen atom the spatial changes in which during the reaction provide valuable clues that facilitate its study. In addition, the C−F analogy is an appropriate complement to the B−E analogy. The pathways for the six reactions were elucidated, and the variation of magnetic susceptibility and its anisotropy along each were examined with a view to assessing the suitability of this aromaticity criterion for discriminating between pericyclic and pseudopericyclic processes. Only the reaction pathways leading to an *E* configuration of the imine were studied in reactions E and F as the *Z* configuration required an orientation of the lone pair in the heteroatom that ruled out its effective involvement in a possible disconnection.

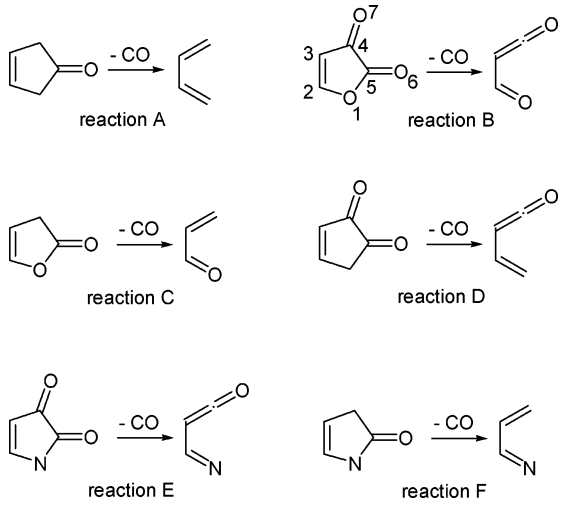

FIGURE 1. Reaction scheme for the decarbonylations studied.

Computational Details

The geometry of each stationary point was fully optimized using the Gaussian98 software package[29] with the 6-31G** basis set and the density functional theory (specifically, the Becke3LYP functional).[30,31] All points were characterized as minima or transition structures by calculating the harmonic vibrational frequencies, using analytical second derivatives. Also, the pathway for each reaction was obtained by using the intrinsic reaction coordinate (IRC) with mass-weighted coordinates.[32−34] Although the evaluation of the absolute aromaticity

(22) Herges, R.; Jiao, H.; Schleyer, P. v. R. *Angew. Chem., Int. Ed. Engl.* **1994**, *33*, 1376.
(23) Jiao, H.; Schleyer, P. v. R. *J. Org. Phys. Chem.* **1998**, *11*, 655−662.
(24) Manoharan, M.; De Proft, F.; Geerlings, P. *J. Org. Chem.* **2000**, *65*, 7971−7976.
(25) Manoharan, M.; De Proft, F.; Geerlings, P. *J. Chem. Soc., Perkin Trans. 2* **2000**, 1767−1773.
(26) Herges, R.; Geuenich, D. *J. Phys. Chem. A* **2001**, *105*, 3214−3220.
(27) Herges, R.; Papafilippopoulos, A. *Angew. Chem., Int. Ed.* **2001**, *40*, 4671−4674.
(28) Kimball, D. B.; Weakley, T. J. R.; Herges, R.; Haley, M. M. *J. Am. Chem. Soc.* **2002**, *124*, 13463−13473.
(29) Frisch, M. J.; Trucks, G. W.; Schlegel, H. B.; Scuseria, G. E.; Robb, M. A.; Cheeseman, J. R.; Zakrzewski, V. G.; Montgomery, J. A., Jr.; Stratmann, R. E.; Burant, J. C.; pprich, S.; Millam, J. M.; Daniels, A. D.; Kudin, K. N.; Strain, M. C.; Farkas, O.; Tomasi, J.; Barone, V.; Cossi, M.; Cammi, R.; Mennucci, B.; Pomelli, C.; Adamo, C.; Clifford, S.; Ochterski, J.; Petersson, G. A.; Ayala, P. Y.; Cui, Q.; Morokuma, K.; Malick, D. K.; Rabuck, A. D.; Raghavachari, K.; Foresman, J. B.; Cioslowski, J.; Ortiz, J. V.; Baboul, A. G.; Stefanov, B. B.; Liu, G.; Liashenko, A.; Piskorz, P.; Komaromi, I.; Gomperts, R.; Martin, R. L.; Fox, D. J.; Keith, T.; Al-Laham, M. A.; Peng, C. Y.; Nanayakkara, A.; Gonzalez, C.; Challacombe, M.; Gill, P. M. W.; Johnson, B. G.; Chen, W.; Wong, M. W.; Andres, J. L.; Head-Gordon, M.; Replogle, E. S.; Pople, J. A. *Gaussian 98*, revision A.9; Gaussian Inc: Pittsburgh, PA, 1998.
(30) Lee, C.; Yang, W.; Parr, R. J. *Phys. Rev. B* **1988**, *37*, 785−789.
(31) Becke, A. D. *J. Chem. Phys.* **1993**, *98*, 5648−5652.
(32) Fukui, K. *Acc. Chem. Res.* **1981**, *14*, 363.
(33) Gonzalez, C.; Schlegel, H. B. *J. Chem. Phys.* **1989**, *90*, 2154.

TABLE 1. Selected Geometrical Parameters of Transition Structures[a]

	TS_A	TS_B	TS_C	TS_D	TS_E	TS_F
X1−C5	2.128 (2.127)	2.090 (2.108)	2.319 (2.261)	2.526 (2.449)	2.099 (2.134)	2.163
C4−C5	2.128 (2.127)	2.046 (1.947)	1.768 (1.769)	1.846 (1.868)	2.140 (1.988)	1.928
X1−C5−O6	132.9 (132.5)	113.3 (114.6)	116.4 (120.7)	128.0 (129.5)	116.1 (118.7)	123.9
C4−C5−O6	132.9 (132.5)	156.4 (153.3)	139.8 (135.6)	143.4 (140.8)	155.4 (150.9)	137.7
C5−X1−C2−C3	−40.1 (−40.9)	0.0 (0.0)	−31.5 (−34.3)	−44.7 (−46.5)	0.0 (0.0)	−38.1
C5−C4−C3−C2	40.1 (40.9)	0.0 (0.0)	50.2 (49.1)	19.7 (20.8)	0.0 (0.0)	43.2
O6−C5−X1−C2	95.8 (92.9)	180.0 (180.0)	91.2 (85.7)	121.8 (116.3)	180.0 (180.0)	91.3
O6−C5−C4−C3	−95.8 (−92.9)	180.0 (180.0)	−67.3 (−71.3)	−126.6 (−122.0)	180.0 (180.0)	−80.6
C5−C3C4O7[b]		180.0 (180.0)		174.7 (175.9)	180.0 (180.0)	

[a] MP2/6-31G* values obtained by Birney et al. are in brackets.[4] Bond lengths are in Å and angles are in deg. [b] Deviation of the C5 atom with respect to the plane formed by atoms C3, C4, and O7.

of a compound remains a controversial, relatively obscure issue,[35] we were primarily interested in its variation during the reaction, and the evaluation of magnetic properties can be a useful tool for this purpose. Changes in magnetic properties along the IRC were monitored at different points for which the magnetic susceptibility (χ) and its anisotropy (χ_{anis}) were calculated. Magnetic susceptibility values were calculated by computing the NMR shielding tensors at the B3LYP/6-311+G(2d,p) level using the IGAIM (individual gauges for atoms in molecules) method,[36,37] which is a slight variation of the CSGT (continuous set of gauge transformations) method.[36−38] Some processes were also monitored by applying the NBO (natural bond orbital) method[18−20] along the IRC, using the B3LYP/6-31G** electron densities. Also we have carried out some ACID calculations (anisotropy of the current-induced density) with the program supplied by Herges.[26] These calculations were performed with the same basis set as the other magnetic properties.

Results and Discussion

It should be noted that the need to determine the whole IRC for each reaction precluded the use of a high computational level. In any case, our results suggest that the chosen level (B3LYP/6-31G**) was more than acceptable. Thus, the activation energy obtained for the prototypical reaction A, zero point energy (ZPE) include, was 48.9 kcal/mol, which is virtually identical with the 49.0 kcal/mol provided by the computationally much more costly MP4(SDTQ)/D95**//MP2/6-31G*+ZPE level[4] and very close to the experimental value (51.3 ± 0.2 kcal/mol).[39] The activation energies for the other reactions were as follows: 21.6 (B), 50.1 (C), 37.4 (D), 36.4 (E), and 60.3 kcal/mol (F). These values are also very similar to those obtained by Birney et al. using the MP4(SDTQ) level.[4] Such excellent consistency had also previously been obtained in DFT calculations for other pericyclic reactions.[40] As can be seen from Table 1, which shows the values of selected geometric parameters, there was a high similarity between DFT and MP2/6-31G* geometries.

Figure 2 shows the energy profiles obtained from the IRC calculations. The whole reaction pathway to the reactants was determined in all cases; that to the products could not be obtained in its entirety as the IRC computations were stopped before the expected complex was reached. In any case, the extent of reaction development examined sufficed for the two molecular fragments to become substantially independent.

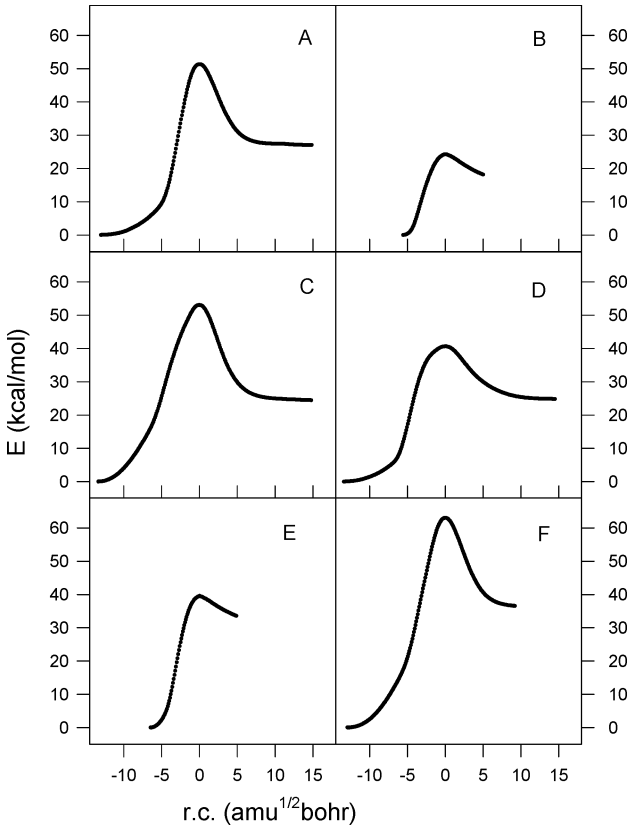

FIGURE 2. Energy profile for the reactions.

Pseudopericyclic reactions are known to exhibit low activation energies.[2−8] This conclusion should be interpreted in a relative rather than absolute manner as, in fact, pseudopericyclic reactions possess low activation energies with respect to analogous pericyclic reactions. When the activation energy of the pericyclic prototype is low, the corresponding pseudopericyclic reaction may even be subject to no activation energy; such is the case with the electrocyclization of 5-oxo-2,4-pentadienal.[17] In the reactions examined in this work, the pericyclic prototype (A) has a high activation energy (48.9 kcal/mol), so the pseudopericyclic reaction can only reach an intermediate activation energy. This is indeed the case with reaction B, unequivocally pseudopericyclic, which

(34) Gonzalez, C.; Schlegel, H. B. *J. Phys. Chem.* **1990**, *94*, 5223.
(35) See Special Issue 5 entirely dedicated to aromaticity: *Chem. Rev.* **2001**, *101*.
(36) Keith, T. A.; Bader, R. F. W. *Chem. Phys. Lett.* **1992**, *194*, 1.
(37) Keith, T. A.; Bader, R. F. W. *Chem. Phys. Lett.* **1993**, *210*, 223.
(38) Cheeseman, J. R.; Frisch, M. J.; Trucks, G. W.; Keith, T. A. *J. Chem. Phys.* **1996**, *104*, 5497.
(39) Dolbier, W. R., Jr.; Frey, H. M. *J. Chem. Soc., Perkin Trans. 2* **1974**, 1674.
(40) Rodríguez-Otero, J. *J. Org. Chem.* **1953**, *18*, 6842.

is subject to a substantial energy barrier (21.6 kcal/mol) that is much lower than that of reaction A in any case. The height of the energy barrier and the shape of the energy profile allow one to draw the conclusions that follow. Thus, reactions C and F behave very similarly to A, which is consistent with a pericyclic nature. The energy barrier of reaction E is not so low as that of B; however, the energy profile of the former is seemingly consistent with a pseudopericyclic nature. Reaction D is the most difficult to interpret: a substantial decrease of the barrier is observed, but also an energy profile that is more similar to those of pericyclic reactions.

In the reactions with the most apparent pseudopericyclic nature (B and E), the pathway between the reactant and the transition state is very short; by contrast, pericyclic reactions involve a much longer pathway and an energy profile that exhibits a more gentle rise at the beginning of the reaction. Based on the calculated geometries, this initial segment of the reaction pathway involves a spatial change but no marked progress in the rupture of the two σ bonds. Thus, the C1−C5 distance in reaction A takes a value of 1.539 Å and remains virtually constant between the reactant (r.c. = −13.01 amu$^{1/2}$bohr) and quite a advanced reaction stage (−5.71 amu$^{1/2}$bohr). Throughout this interval, which encompasses more than half of the pathway to the transition state, the energy rises to only 14% of the barrier. Beyond this point, the energy increases substantially, and so does the C1−C5 distance, which reaches 2.128 Å in the transition state. The pseudopericyclic reactions B and E behave rather differently from the previous one; both the energy and the X1−C5 and C4−C5 distances increase from the start. This can be summarized as follows: whereas pseudopericyclic reactions are "ready" to start, pericyclic reactions require the prior spatial accommodation of the reactants in order to facilitate the bond ruptures involved. Such accommodation essentially involves the migration of the CO group from the molecular plane to a position normal to it. As can be seen in Figure 3, which includes the normal vibrational frequency corresponding to each imaginary frequency, such a migration has been completed by the time the transition state is reached; in fact, at TS_A, the CO group is virtually normal to the remainder of the molecule and the hydrogen atoms bonded to C1 and C4 undergo the disrotatory movement typical of a linear suprafacial reaction (see Figure 4*a*). As can also be seen from Figure 3 (and Table 1), the situation of C and F is very similar to that of A as regards both the position of the CO group and atom movements; however, the lack of one (F) or two hydrogen atoms (C) precludes the confirmation of the disrotatory movement. Figure 3 also shows that the transition states of reactions B and E are completely planar: the CO group departs from the remainder of the molecule but continues to be absolutely coplanar. All of this is consistent with a pseudopericyclic reaction with two disconnections: one at the heteroatom X1 that involves a lone electron pair and the other at C4 that involves the outer π(4−7) bond (see Figure 4*b*). As with the energy profiles, reaction D is the most difficult to interpret as its transition state has the CO group virtually halfway between a coplanar and a normal position. The O6C5X1C2 and O6C5C4C3 dihedrals (Table 1) reflect the position of the leaving CO group: they are

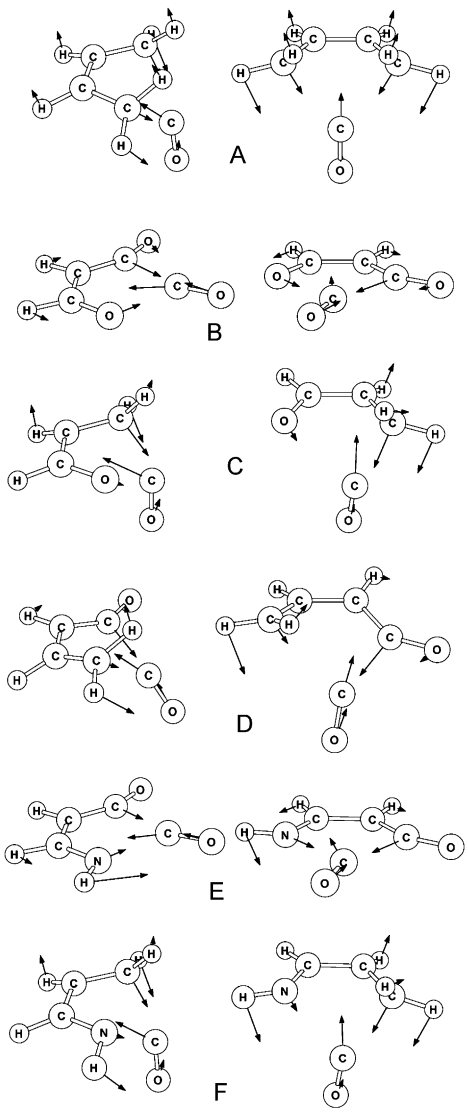

FIGURE 3. Transition structures and normal mode eigenvectors for the coordinate frequency.

close to 90° for TS_A, TS_C, and TS_F, exactly 180° for TS_B and TS_E, and intermediate (in the region of 125°) for TS_D. However, a closer look at the geometry of TS_D reveals that the atom arrangement around C4 is very similar to those in the pseudopericyclic reactions B and E. Thus, C5 departs from C4 and adopts a nearly planar configuration: the angle between C5 and the C3C4O7 plane is ca. 175° (see Table 1). Such a planarity around C4 can also be evaluated from the degree of pyramidalization; a simple way of quantifying it is by defining the planarity defect at C4 as 360° minus the summation of angles around this atom. This yields a value of only 0.12° (0.07° with MP2/6-31G*), which represents nearly absolute planarity. However, as expected, the arrangement around C1 in TS_D is very similar to that in the pericyclic reactions: the C5C1C2C3 dihedral angle is −44.7°, which is very similar to the −40.1° in TS_A. In summary, the transition state of reaction D seemingly exhibits a disconnection at C4. On the other hand, the transition states of C and F are very similar to that of A and the

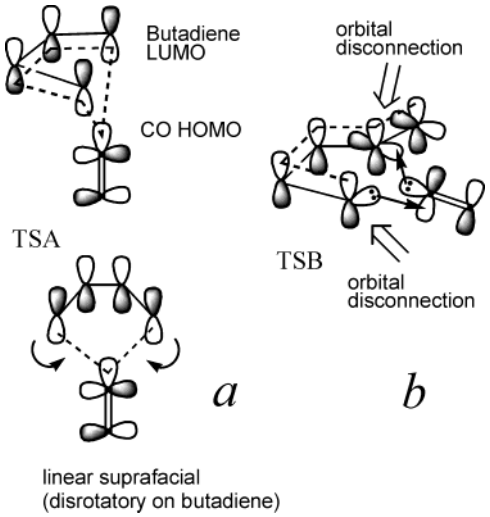

FIGURE 4. (*a*) Orbital interactions in the pericyclic decarbonylation A. The CO is under the butadiene plane. There is a cyclic orbital overlap around the ring of interacting atoms. (*b*) Orbital interactions in the pseudopericyclic decarbonilation B. All of the atoms are coplanar. There are orbital disconnections where the out-of-plane and in-plane sets of orbitals meet at a single atom. In both figures, the departing CO is drawn hybridized as carbon monoxide, with the carbon lone pair and one π^* orbital shown.

C5X1C2C3 dihedrals in the former (−31.5° for TS_C and −38.1° for TS_F) are very similar to that in TS_A (−40.1°). Because this dihedral angle somehow reflects a possible disconnection at X1 (the angle is 0° in pseudopericyclic reactions), the occurrence of such a disconnection in TS_C and TS_F is more dubious.

Figures 5 and 6 show the variation of the magnetic properties studied during the reactions. The prototypical pericyclic reaction A is consistent with the expected pattern: marked aromatization near the transition state that reflects in the presence of well-defined minima in the curve for both magnetic susceptibility (χ) and its anisotropy (χ_{anis}). The curves for reactions C and F are highly consistent with this pattern, particularly as regards χ_{anis}. The behavior of reactions B and E is typical of definitely pseudopericyclic reactions, i.e., processes involving no aromatization near the transition state. Thus, the magnetic susceptibility decreases steadily from reactant to products, and its anisotropy exhibits a small maximum near the transition state. In addition, the curves for B and E are virtually identical, which suggests that the presence of an oxygen or nitrogen atom at position 1 is insubstantial. As with the structural parameters, reaction D is the most difficult to interpret. The curves for this reaction are obviously not so clearly pseudopericyclic as those for B and E; however, they clearly depart from a pericyclic pattern (the decarbonylation appears to involve no aromatization). Consequently, on the basis of Figures 5 and 6, reaction D should be classified as pseudopericyclic, which is consistent with the above-described planarity around C4 in the transition state. To support this conclusion, we performed an additional computation involving the obtainment of a forced pseudopericyclic transition state for reaction D; to this end, we used a restricted optimization in which all atoms in the molecule except C1 and its two hydrogen

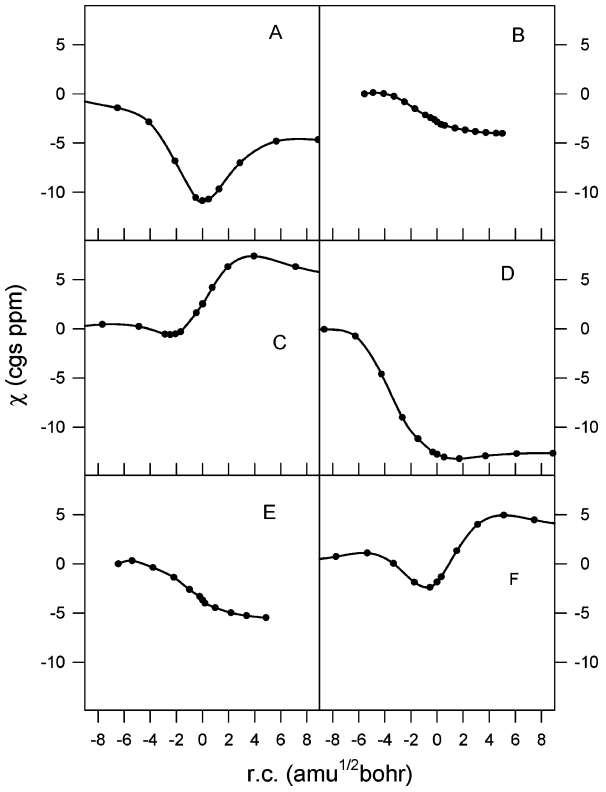

FIGURE 5. Variation of magnetic susceptibility realtive to the reactant.

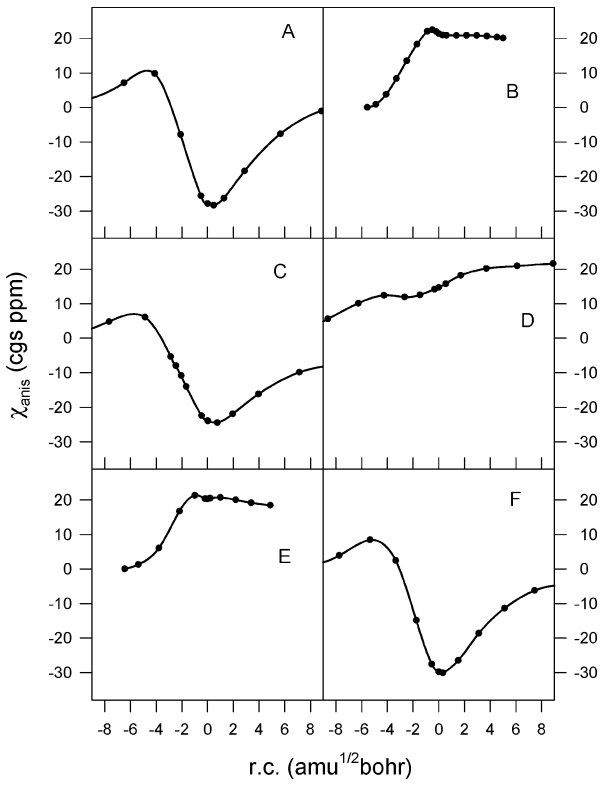

FIGURE 6. Variation of anisotropy of the magnetic susceptibility relative to the reactant.

atoms were forced to remain in the plane. The result was a structure essentially similar to the true TS_D with an energy only 2.8 kcal/mol higher; the activation energy

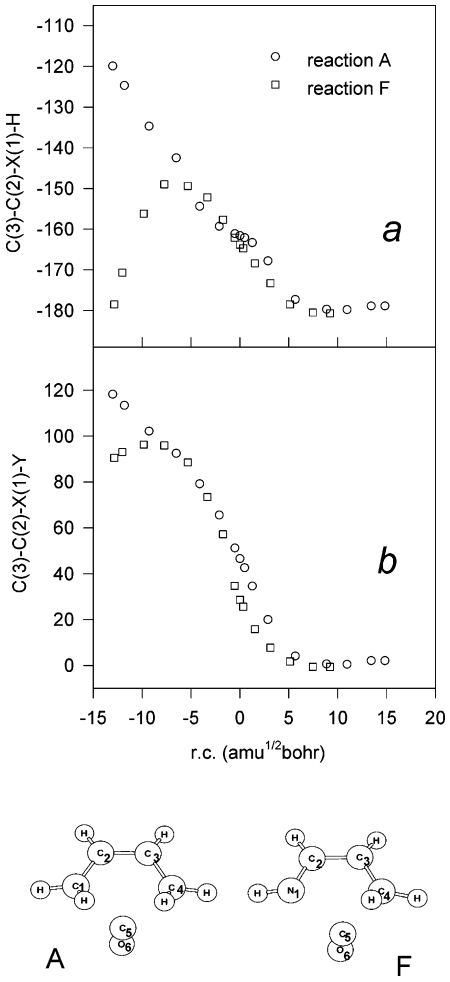

FIGURE 7. (*a*) Change of the C3−C2−X1−H dihedral angle along the A and F reactions. For reaction A, hydrogen atom refers to the outer one on C1. (*b*) Change of the C3−C2−X1−Y dihedral angle along the A and F reactions. Y denotes the lone pair of N1 in reaction F and the inner hydrogen atom of C1 in reaction A.

thus rose from 37.4 to 40.2 kcal/mol, which was still much lower than the value for the prototypical pericyclic reaction.

A global analysis of our results leads to the following conclusions: reactions A, C, and F are definitely pericyclic; reactions B and E are pseudopericyclic and involve two disconnections; and reaction D is also pseudopericyclic but involves a single disconnection. So far, everything is consistent with the assignations of Birney et al. However, there is one clear discrepancy as these authors state that reaction C is essentially pericyclic even though it exhibits a disconnection at O1. We believe such a disconnection does not occur; in fact, one must not confuse a possible disconnection with an actual disconnection. Thus, although the oxygen atom possesses lone electron pairs that might give rise to such a disconnection, our results suggest that this is not the case, so the reaction is essentially a normal pericyclic one. This situation was previously observed in the electrocyclization of (2*Z*)-2,4,5-hexatrienal and (2*Z*)-2,4,5-hexatrien-1-imine, where the participation of the lone pair oriented toward the inside of the ring and hence involved in the cyclization does not seem to suffice to suppress the essential features of a

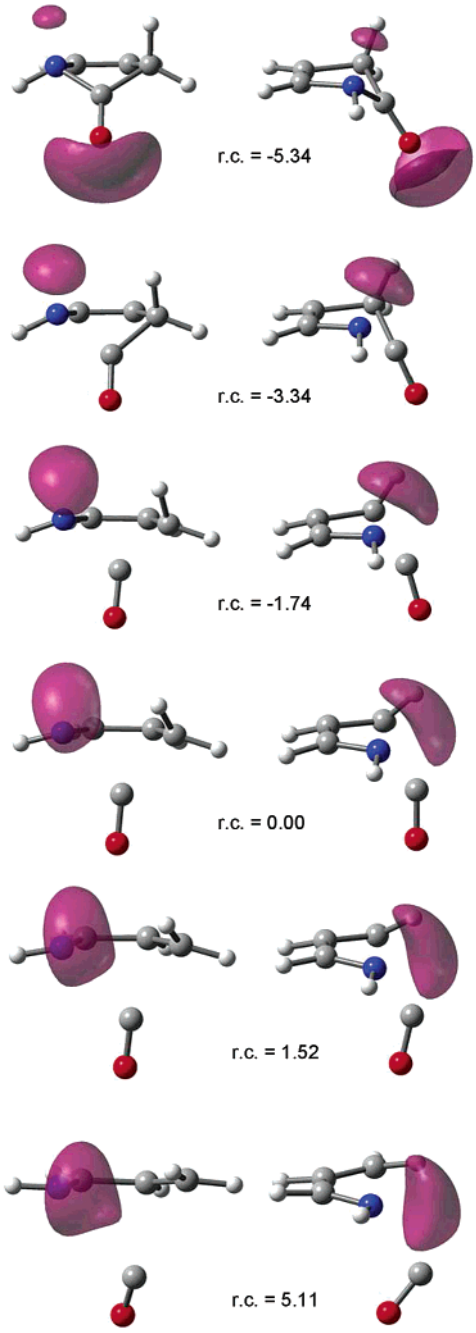

FIGURE 8. Electrostatic isopotential surfaces (−0.05 au) at various points along the F reaction pathway.

pericyclic reaction.[17] The occurrence of a disconnection at O1 would preclude rotation about the C2O1 bond. The problem here is that the oxygen atom has no bonded hydrogen atoms enabling to study the rotation. This problem can be partly circumvented by examining the isoelectronic reaction F, where the nitrogen atom possesses a properly (inward) oriented lone pair in addition to a hydrogen atom the position of which along the reaction pathway can be monitored. In Figure 7 the rotation of the C2X1 bond is analyzed for reactions A and F. For this purpose Figure 7a compares the variation of the C3C2X1H dihedral (based on the outer hydrogen atom for reaction A) and Figure 7b compares the variation of the C3C2X1Y dihedral (Y denotes the lone pair of

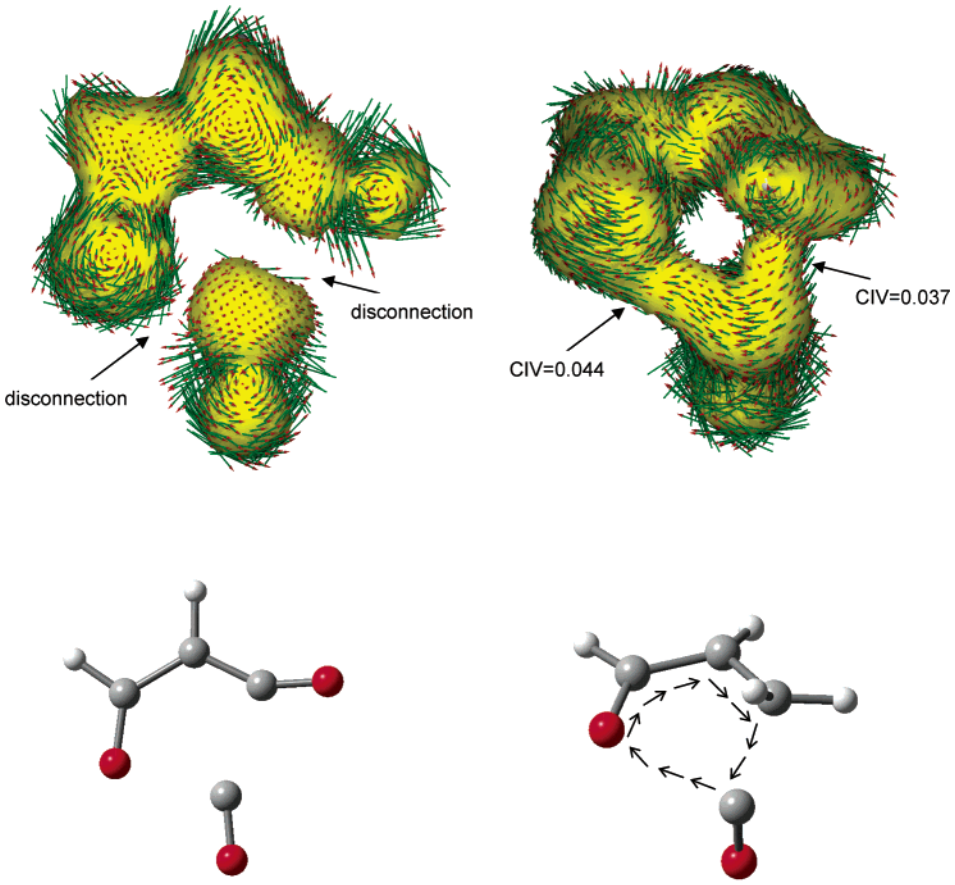

FIGURE 9. ACID plots for the transition states of reactions B and C. The current density vectors (green arrows with red tips) are plotted onto the isosurface of value 0.025. In TS_C these vectors exhibit a closed circle in the five-membered ring and no disconnection. In TS_B the topology of delocalized electrons exhibits two clear disconnections.

N1 in reaction F and the inner hydrogen atom of C1 in reaction A). The directionality of the lone pair is measured with the NBO calculation. Figure 7 shows that reactions A and F behave very similarly. Only at the very beginning of the reaction, up to a reaction coordinate value of ca. −7 amu$^{1/2}$bohr, is there a clear disparity. This difference is easily attributable to the different structure of reactant: in A the C1 is bonded with sp^3 hybridization and in F the N1 is bonded with sp^2 hybridization (the hydrogen atom is coplanar, whereas the lone pair is normal to the plane and forms a hybrid of virtually pure p_z character). Therefore, the rotation about the C2X1 bond behaves very similarly in reactions A and F. In our opinion, this indicates the absence of disconnection at N1 in reaction F since it is at this position that the typical rotation of pericyclic processes (disrotation with respect to C4) takes place. Figure 7b may be challenged on the grounds that we used the NBO method throughout the IRC on a "nonclassical" chemical species (one with half-broken bonds). The NBO procedure is intended to provide a description of the electronic structure in terms of localized bonds and lone pairs, corresponding to a single classical Lewis formula, but this is obviously problematic for a species that is not a minimum. Because the NBO procedure involves a compromise, the chemical significance of the results of this analysis should not be overrated. For this reason, to confirm the rotation of N1 in reaction F, we performed calculations with a view to obtaining an unambiguously defined quantum mechanical quantity, namely, the molecular electrostatic potential (MEP). Figure 8 shows the isopotential surfaces (−0.05 au) at various points along the reaction pathway. As can be seen, the zones with a negative potential are clearly related to the presence of the lone pairs in the heteroatoms (N and O). As the reaction develops, the zone with the most negative electrostatic potential shifts from O6 to N1; in fact, the zone for O6 in the figure only appears when the reaction coordinate is −5.34 amu$^{1/2}$bohr, while that for N1 increases in size. As can clearly be seen, the N1 zone rotates from a position normal to the molecule to one absolutely coplanar with the 2-propen-1-imine fragment. This rotation is completely identical with that observed in the localization of the lone pair provided by the NBO calculations. We thus believe NBO and MEP calculations show that the rotation of N1 in reaction F is comparable to that of C1 in the unequivocally pericyclic reaction A. Also, on the basis of the similar behavior of the structural and magnetic properties of F and C, the latter reaction must also be a normal pericyclic reaction involving absolutely no disconnection.

To corroborate the inexistence of disconnections in the reaction C we have also applied the ACID method.[26−28] This method is an efficient tool for the investigation and visualization of delocalization and conjugation. A cyclic topology in an ACID plot indicates a pericyclic reaction. Disconnections that are characteristic for pseudopericyclic systems are immediately visible by a disconnection in the contiguous system of the ACID boundary surface.

Figure 9 presents the ACID isosurface of the transition structures for the reactions B and C. TS_C does not exhibit any disconnection. Moreover, the current density vectors plotted onto the isosurface show the pericyclic nature of the delocalized system: the diatropic ring current forms a loop around the five-membered ring as expected for an aromatic system. The extent of conjugation can be quantified by giving the critical isosurface value, CIV, at which the topology of the ACID boundary surface changes. Although the values for the two breaking bonds are not very large (0.037 and 0.044), they show a substantial conjugation. To show the clear difference, Figure 9 also contains the plot corresponding to a reaction unequivocally pseudopericyclic. In contrast to TS_C, TS_B shows two clear disconnections for the two breaking bonds.

In summary, we agree with Lemal's original statement that a single disconnection suffices to induce a pseudopericyclic process,[1] though in some cases these are not easily defined. In any case, the occurrence of two disconnections gives rise to processes that are easier to classify as unequivocally pseudopericyclic.

Conclusions

We used the variation of energy, structural, and magnetic parameters along the reaction pathway with a view to examining various thermal cheletropic decarbonylations. On the basis of the results, reactions C and F behave identically with the prototypical pericyclic reaction A. These three reactions share the following essential features: high activation energies, transition structures with a CO group normal to the remainder of the molecule, and marked aromatization near the transition state. On the other hand, reactions B and E behave like pseudopericyclic processes; thus, they exhibit lower activation energies, fully planar transition structures, and no aromatization. Reaction D is the most difficult to classify as it lies between the previous two extremes. In any case, a careful study of its characteristics allows it to be classified as pseudopericyclic as it exhibits no appreciable aromatization and involves a likely disconnection at C4 due to the participation of the outer π bond. This classification is consistent with that previously reported by Birney et al.[4] However, there is a serious discrepancy in the assignation of the number of disconnections. Thus, while these authors claim that a pericyclic reaction (C) may involve a disconnection, our results suggests that it does not. Therefore, consistent with Lemal's original definition,[1] we believe that a pseudopericyclic reaction involves one or more disconnections, whereas a pericyclic reaction involves none. Hence the possibility of a disconnection does not necessarily imply its occurrence or that of a pseudopericyclic reaction as a result.

As confirmed by the results, the variation of magnetic properties (viz. magnetic susceptibility and its anisotropy) along the reaction pathway is a useful tool for discriminating between pericyclic and pseudopericyclic reactions. Thus, the former, unlike the latter, exhibit well-defined minima near the transition state.

Acknowledgment. The authors thank the Xunta de Galicia (Project PGIDIT02PXIA20901PR) for financial support. The authors express their deep gratitude to Dr. Herges for his assistance and for the ACID program.

Supporting Information Available: Listings of energy, ZPE, geometries, and frequencies for each transition structure. This material is available free of charge via the Internet at http://pubs.acs.org.

JO034526O